Article

Insights into the Characterization of the Self-Assembly of Different Types of Amphiphilic Molecules Using Dynamic Light Scattering

Aicha Kadiri, Teffaha Fergoug, Khaled O. Sebakhy,* Youcef Bouhadda, Rachida Aribi, Fatima Yssaad, Zineeddine Daikh, Mustapha El Hariri El Nokab, and Paul H. M. Van Steenberge

Cite This: ACS Omega 2023, 8, 47714−47722

Read Online

ACCESS | Metrics & More | Article Recommendations

ABSTRACT: The self-assembly of cetyltrimethylammonium bromide, sodium dodecyl-sulfate, Triton X-100, and sulfobetaine surfactants in aqueous solutions was examined by dynamic light scattering, both in the presence and absence of 0.1 M NaCl salt, across various temperatures. For each surfactant, critical parameters, such as concentration and phase transition temperatures, of micelles were determined by monitoring changes in the hydrodynamic diameter with concentration and temperature. Additionally, we explored the self-assembly behavior of these surfactants when they are introduced alongside polystyrene nanoparticles. Our findings enabled the elucidation of surfactant molecule adsorption mechanisms onto polystyrene nanoparticle surfaces. Furthermore, by analyzing variations in the z-average diameter and zeta potential, we were able to establish the Krafft point, a parameter that remains imperceptible when polystyrene nanoparticles are absent from the solution.
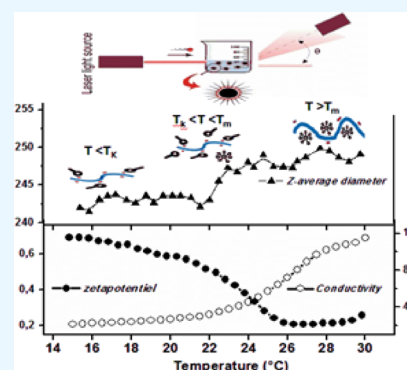
1. INTRODUCTION

Surfactants find extensive applications in various industries. They exhibit pronounced surface activity, readily adsorbing onto air−water or oil−water interfaces. This behavior arises from their inherent amphiphilic nature, featuring a hydrophobic tail at one end and a hydrophilic head at the opposite end.[1] Upon dissolution in aqueous media, and above their CMC, surfactant molecules undergo self-assembly, forming micelles that minimize water−oil interactions.[2]

The CMC is notably influenced by thermodynamic parameters, including temperature, ionic strength, and additives. In the case of ionic surfactants, their solubility significantly increases beyond the CMC when the temperature reaches the Krafft temperature (T_k).[3] The T_k marks the point at which previously insoluble, hydrated surfactant crystals begin to melt, integrating into the bulk solution as either micelles or free surfactant molecules. The temperature at which the final hydrated crystal dissolves is referred to as the melting temperature (T_m), with its value being contingent on concentration. While the thermodynamic phase separation model (PSM) equates T_k and T_m, the mass action model (MAM) discerns a distinction between them.[4] Conversely, non-ionic surfactants lack defined Krafft or melting points. Instead, a cloud temperature (T_c) characterizes the temperature at which a solution turns turbid upon temperature elevation for a given surfactant concentration.[5]

Broadly speaking, the aqueous dissolution process of a surfactant solution is governed by the equilibrium of the adsorption, micel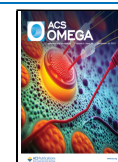lization, and solubility. These phenomena are contingent upon factors such as the characteristics of the hydrophobic chains, the counterion species, concentration, and temperature.[6,7] Thus, studying the dissolution dynamics of surfactants and tracing the evolution of their phase diagrams through various thermodynamic coordinates are a necessary task. The best techniques among few others, which are thought to yield simultaneously insights into parameters like CMC and T_k, T_m, or T_c, are calorimetry and thermal conductivity for charged surfactants.[8,9] Other techniques such as small-angle scattering techniques (e.g., neutron SANS and X-ray SAXS) and light scattering methods (e.g., static SLS and dynamic DLS) are better used to explore the CMC, micelles size, and morphology.[10,11] DLS rarely tackles the thermodynamic parameters due to the electrical charges carried by micellar systems, which complicate the interpretation of scattering experiments.[12] To overcome this, a majority of dynamic light scattering (DLS) investigations concerning micellar solutions have been conducted in the presence of significant salt concentrations. For example, Mazer et al.[13] delved into the static and dynamic light scattering of aqueous sodium dodecyl sulfate (SDS) solutions with varying NaCl concentrations. Their findings revealed the progression from spherical to rod-

like micellar structures as salt concentration increased (NaCl $\leq$ 0.45 M).[13,14] A similar behavior emerged in a 0.01 mol L^{-1} solution of CTAB, where spherical micelles transitioned to worm-like micelles with increasing KBr salt concentrations.[15] Rohde and Sakmann[16] observed an aggregation number shift in SDS micelles from $N = 27$ to $N = 95$ as NaCl concentration rose from 0 to 0.05 mol L^{-1}. Notably, micelle form transformations were noted beyond a salt concentration of 0.2 mol L^{-1}. The rationale behind the use of salt is to mitigate the formation of extensive and intricate water/surfactant-clustered structures, which can often impede accurate interpretation of DLS data pertaining to micellar size distribution.[17] Unfortunately, the determined critical micelle concentration (CMC) values are influenced by the concentration of salt present.

To circumvent these DLS limitations, another promising alternative involves the utilization of polystyrene polymer nanoparticles as additives instead of salts. These nanoparticles possess exceptional monodispersity and do not provoke water clustering, thereby circumventing hindrance to the micellization process. In this context, it is worth noting that the polymer surfactant combination has been studied for a long time as evidenced by the number of publications dedicated to this tandem.[18−20] If initially a lot of work focused on the stability side of the colloidal complex they form together, other aspects related to their uses in different industrial fields as cosmetics, recovery of oils, drug delivery, and more[21,22] have taken over time. So, aspects such as surfactant/polymer adsorption mechanisms, spatial structure of the polymer surfactant complex, and their rheology dominate the research conducted nowadays.[23−25]

Dynamic light scattering combined with surface adsorption experiments are techniques frequently adopted to characterize polymer surfactant complexes[18−25] usually above melting temperature of the surfactant for application purposes. Interestingly, in the context of dynamic light scattering (DLS) measurements, only a limited number of studies have expanded their investigations to determine micellar phase transition temperatures, such as the Krafft temperature.[26] This prompted us to allocate significant attention to this aspect. This study presents an innovative approach that entails investigating the impact of temperature on polymer−surfactant interactions. Through this approach, it becomes feasible to deduce crucial transition temperatures for surfactant systems, particularly those with electrically charged components that pose challenges for DLS analysis. Notably, our work marks the first instance in which polystyrene polymer nanoparticles are synergistically employed with surfactants to extract the Krafft temperature, melting temperature, and CMC of distinct micellar species. Consequently, this study examines a diverse array of surfactants (as depicted in Scheme 1) through dynamic light scattering, encompassing variations in both concentration and temperature. The influence of polystyrene nanoparticles (PSNP) on micellar properties is systematically investigated and subsequently discussed.

2. EXPERIMENTAL PART

2.1. Reagents. Sodium dodecylsulfate (SDS) (99%), cetyltrimethylammonium bromide (CTAB) (99%), Triton X-100 (TX-100) (99%), and sulfobetaine 16 (SB3-16) (98%) were obtained from Sigma-Aldrich and used as received. The polystyrene sample used was from a standard solution provided by Malvern Panalytical, containing highly uniform polystyrene

Scheme 1. Chemical Structures of the Surfactants Investigated in the Present Work
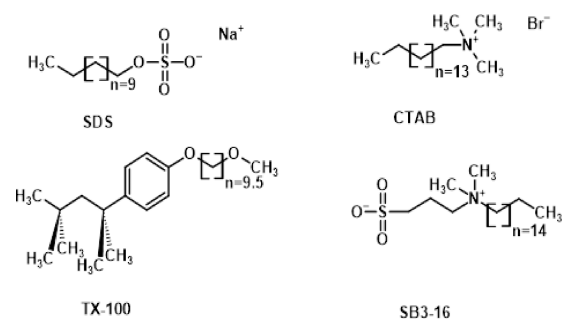
spheres calibrated by NIST-traceable standards with a nominal diameter of 220 nm and a zeta potential of −45 mV in pure water. Sodium chloride (99.8%) was purchased from LOBA Chemie.

2.2. Dynamic Light Scattering (DLS) and Zeta Potential (Z_p) Measurements. Dynamic light scattering experiments were performed on a Zetasizer Nano-ZS model 3600 (Malvern Instruments, UK) equipped with a He-Ne laser ($\lambda = 633$ nm, 4.0 mW) at an angle of 173°. The time-dependent correlation function was measured at different temperatures for different concentrations of surfactants above their respective CMC in water in the presence and absence of NaCl and was analyzed in cumulative mode using the integrated Zetasizer software. The instrument software (Malvern Zetasizer software v.7.11) provides three different alternatives to quantify the size distribution based on intensity, volume, or number. The zeta potentials of the samples prepared in our work were determined using electrophoretic mobility measurements based on the laser Doppler velocimetry method with the phase analysis light scattering (PALS) option.[27] All results are the average from at least three measurements in each one.

3. RESULTS AND DISCUSSION

3.1. Size Distribution of Different Types of Micelles and Effect of Salt on Their Size Distribution. Figure 1 depicts the size distribution by intensity, volume, and number for 8×10^{-2} M SDS, 10^{-2} M CTAB, 3×10^{-3} M TX-100 at 298 K, and 10^{-4} M SB3-16 at 313 K for aqueous solutions with 0.1 M NaCl salt (dashed line) and without NaCl (continued line). First, for free salt solutions, every size distribution by intensity exhibits a multipeak feature where the first peak on every distribution (centered on 1.8 nm for SDS, 5.5 nm for CTAB, 7.2 nm for TX-100, and 6.5 nm for SB3-16) represents the hydrodynamic diameter of the assumed classical Hartley-type micelles. All obtained values are close to the ones previously reported elsewhere by DLS, SAXS, and SANS techniques or are of the same order.[8,28]

For the other remaining peaks in Figure 1, Mirgorod et al.[17] identified them in terms of association of monomer/micelle species with two types of water-structured clusters. These authors performed SANS, SAXS, and DLS experiments on the SDS/water system above the CMC and deduced that besides the classical SDS micelles, there may exist entities made of monomers/micelles associated with clustered water molecules as low-density level (LDL) clusters or as high-density level (HDL) ones.[17] Despite these peaks disappearing when using volume or number size distributions as shown in Figure 1,
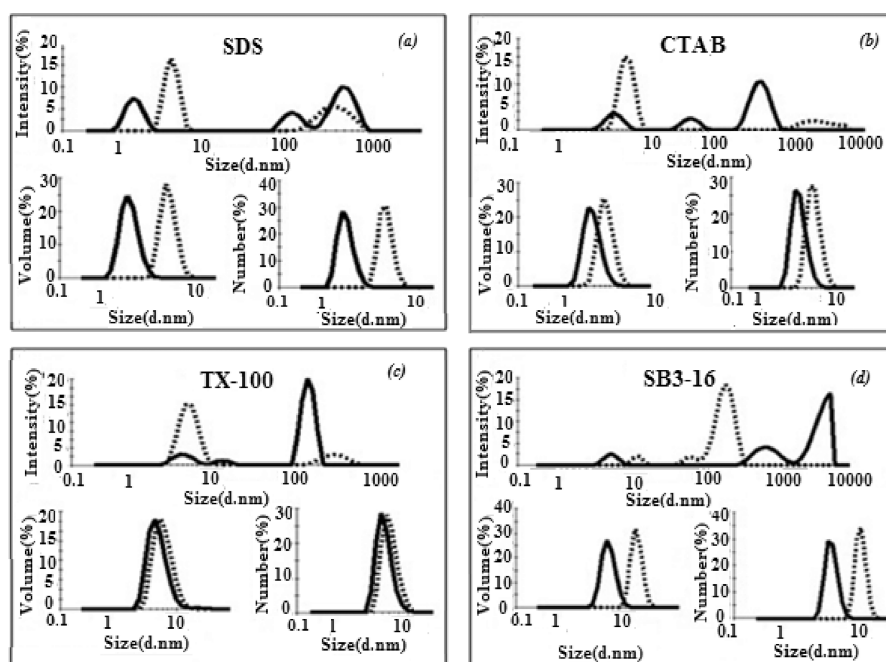
Figure 1. Size distribution by intensity, volume, and number for (a) 8×10^{-2} M SDS, (b) 10^{-2} M CTAB, (c) 3×10^{-3} M TX-100 at 298 K, and (d) 10^{-4} M SB3-16 at 313 K without NaCl (continued line) and with 0.1 M NaCl (dashed line).

these authors recommend keeping them in mind for the ionic surfactant case, when the z-average diameter is considered instead of hydrodynamic diameter (d_h).

In DLS analysis, the intensity distribution is the preferred representation for particle size distribution because it is the closest distribution to what is measured, but it is commonly interesting to check qualitatively the number size distribution. In fact, number distributions emphasize the species with the highest number of particles present in solution, key information in our research since micelle behavior is our main task of interest. According to the volume-based size distribution, our surfactant solutions (with concentrations around 10 times the CMC of the corresponding surfactant) are dominated by a population of micellar nanoparticles with sizes of approximately 1.6, 4.7, 7.1, and 5.9 nm for SDS, CTAB, TX-100, and SB3-16, respectively.

The same trend is obtained when the size distribution is expressed by number mode, where results show again that the surfactant solutions are composed mainly and not exclusively of a population of nanoparticles with hydrodynamic diameters of about 1.4, 4.1, 6.2, and 5.4 nm, respectively. Table 1 summarizes the obtained data.

For the salt effect analysis, only the first peak (Figure 1a−d) for each surfactant is considered. It is easy to note that for the ionic surfactants SDS, CTAB, and SB3-16 micelles (Figure 1a,b,d), the hydrodynamic diameter increases with the addition of NaCl salt (dashed line). This variation derives from the decrease in the electric repulsion of the head groups, which facilitates the aggregation of the monomers and leads to the increase in the size.[2,17] On the other side (Figure 1c), when the salt is added to the TX-100 surfactant solution, the increase in the micelle size is not as large as shown with ionic surfactants. Since TX-100 is a non-ionic species, the main force responsible for the variation of the micelle size is the dehydration,[29,30] a process that induces a smaller headgroup area and, therefore, a slight change in micelle size.

Second, when the salt is added, the intensity of light scattered by LDL or HDL water clusters decreases notably except for SB3-16. Thus, the electrostatic field created by the added salt ions seems to eliminate water density variations and aids the surfactant molecules to separate from their water clusters and form typical micelles,[17] and therefore, the number of surfactant + LDL and surfactant + HDL scatters is substantially decreased. These observations are in agreement with observations reported elsewhere,[17] which underline that the surfactant−water clusters disappear with addition of salts especially for the monocharged ones.

The PDI parameter, which represents the polydispersity index of the nanoparticles in solution, is reported in Table 1. The PDI values decrease as the amount of the added salt or surfactant concentration increases, underlying the utility of working at high surfactant concentration and in the presence of salt. The interesting observation is that for SB3-16 and TX-100 surfactants, at low surfactant concentrations, the presence of salt is mandatory to decrease the PDI value, whereas for higher ones, its contribution is limited.

3.2. Effect of Concentration and Temperature on Size Distribution of Micelles. Figure 2 shows the variation of hydrodynamic diameter of SDS, CTAB, TX-100 (at 298 K), and SB3-16 (at 313 K) micelles as a function of surfactant concentration with and without 0.1 M NaCl.

It is evident that as long as the concentration is lower than the critical micelle concentration, no signal is obtained since no micelles are formed, but when the concentration exceeds the CMC, a signal is detected and the corresponding micelle hydrodynamic diameter is deduced.[31] These values are in accordance with ones already reported by Peter et al. and others.[1,-5,32] For all salt free surfactant solutions, the micelle size remains almost constant or slightly decreases within the studied concentration range, below 10 times the CMC. These values and behaviors are again in good agreement with ones reported in the literature[13,15,17] as shown in Table 2.

Table 1. Polydispersity Index, Intensity, and Hydrodynamic Diameter Values by Intensity, Volume, and Number in the Absence and Presence of 0.1 M NaCl and in the Presence of Polystyrene for the Different Micellar Solutions

salt and surfactant concentrations	PDI	d_h by intensity (nm)	intensity (%)	d_h by volume (nm)	d_h by number (nm)
8×10^{-2} M SDS	0.60	1.8	29.5	1.6	1.4
		128.3	18.4		
		488.2	52.1		
8×10^{-2} M SDS + 0.1 M NaCl	0.40	4.9	56.2	4.5	4.1
		402.4	40.5		
		5377	3.2		
10^{-2} M CTAB	0.50	5.5; 3.5[7]	20	4.7	4.1
		55.43	13.4		
		445.3	66.6		
10^{-2} M CTAB + 0.1 M NaCl	0.30	8; 7.8[7]	97.5	7.1	6.4
		2677	20.5		
3×10^{-3} M TX-100	0.50	7.2	14.1	7	6.2
		20.8	4.3		
		226.2	81.6		
3×10^{-3} M TX-100 + 0.1 M NaCl	0.25	8.3	80.8	6.4	5.8
		484.4	16.8		
		5449	2.5		
0.08 M TX-100	0.17	10.8	100	10.2	9.6
0.08 M TX-100 + 0.1 M NaCl	0.14	11.7	100	9.8	8.2
10^{-4} M SB3-16 at 313 K	0.90	6.5	8.6	5.9	5.4
		820.5	26.6		
		4313	64.8		
10^{-4} M SB3-16 + 0.1 M NaCl at 313 K	0.74	13.7	5.2	13	12.3
		79.5	7.3		
		220.1	87.6		
0.1 M SB3-16 at 313 K	0.24	9.2	100	7.3	6.2
0.1 M SB3-16 + 0.1 M NaCl at 313 K	0.21	6.1	87.2	5.5	4.9
		238.8	12.8		

For all studied surfactants, the presence of NaCl in aqueous solutions causes a decrease in CMC and an increase in micelle size values (see arrows on Figure 2), which is primarily due to a reduction in the electrostatic repulsion between polar head groups in the presence of the excess counterions of the salt, as argued in several studies.[4,17]

Figures 2e shows, for SDS, the variation of the hydrodynamic diameter as a function of temperature and added NaCl at a concentration 10 times that of CMC. In the absence of salt and at a low temperature region $T < 17$ °C, the hydrodynamic diameter d_h value is not measurable, but at $T > 17$ °C, d_h increases sharply, which coincides with the known SDS melting temperature T_m (PSM).[4] At more elevated temperatures, d_h values stabilize around 1.5 nm. When the salt is added to the solution, both T_m and micelle size values shift toward greater values as shown in Figure 2e, in accordance to other published studies[13,29] and the general trend already observed for free salt solutions is obtained.

For TX-100, at a concentration 10 times the CMC, no salt effect is revealed, and the hydrodynamic diameter variation is almost identical between the pure surfactant solution and the salted one. The hydrodynamic diameter d_h grows gradually with temperature around 10 nm before increasing dramatically to reach almost 190 nm at $T = 55$ °C, where the solution separates into two phases. From $T_c = 55$ to 60 °C, the

destruction of hydrogen bonds between the polyethylene oxide (PEO) chain of the TX-100 surfactant and water occurs intensively and attractive interactions (dipole–dipole interactions) increase, resulting in micellar development.[30] As a result, phase separation is induced by an increase in d_h and micelle coalescence.

For CTAB surfactant solution at a concentration 10 times of CMC, the variation of the hydrodynamic diameter as a function of temperature in the absence of NaCl is similar to the one observed with SDS. Thus, $T_m = 25$ °C should correspond to the melting temperature for this surfactant, but when NaCl salt is added, the CTAB micelles seem to exist along the studied temperature range, and the T_m decreased to reach $T = 20$ °C. This behavior was also reported by Roy et al.[33] who noted that for CTAB surfactant aqueous solution, the addition of 0.01 M NaCl induces a dramatic decrease in T_m, which shifts from $T = 25$ °C to $T = 16$ °C for 0.1 M CTAB aqueous solution. The argument proposed by the same author[33] stated that the presence of a Cl⁻ ion increases the concentration of free water molecules in the bulk and induces a salting-in effect. As a result, the solubility of CTAB increases in the presence of Cl⁻ because of an increase in hydration of the surfactant with a consequent decrease in the T_k.[33]

For the SB3-16 surfactant at a concentration 10 times that of CMC, the addition of NaCl induces a decrease in hydrodynamic diameter values along with increasing temperature and a little bump is observed around $T_m = 35$ °C, revealing its probable melting temperature, but this value diminishes to $T_m = 32$ °C when NaCl is added, an opposite behavior with regard to the SDS surfactant. This may mean that the SB3-16 surfactant behaves as a cationic surfactant under these experimental conditions.

3.3. Effect of the Concentration of Different Surfactants on the Size Distribution of Polystyrene.

The variation in the z-average diameter (z_{ave}-d) of the polystyrene nanoparticle PSNP, as well as the related change in the zeta potential (Z_p) as a function of concentration of the surfactant, is illustrated in Figure 3a–d for SDS, CTAB, TX-100 ($T = 298K$), and SB3-16 ($T = 313K$), respectively.

For all surfactants, an initial little variation in z_{ave}-d values at low concentration below the surfactants' CMCs is observed followed by a substantial increase to a maximum and, finally, a decrease to an approximately constant level above $C \approx$ CMC. The zeta potential variations are sensitive to the average diameter variation, especially for SDS, TX-100, and CTAB surfactants, but relatively negligible for the SB3-16 one.

The obvious explanation is that at low concentrations just below the surfactants' CMCs, the surfactant molecules first adsorb onto the polystyrene particles by hydrophobic/electrostatic interaction; however, since the hydrophobic tails of the surfactant also carry ionic or polar groups depending on the surfactant type, the zeta potential of the nanoparticle is systematically affected. In Figure 3a, at low surfactant concentrations ($<$CMC$_{SDS}$), the negative charge on the PSNP increases slightly because the SDS surfactants and the polystyrene surface both carry negative charges. Hereby, we expect that SDS negative ions will be repelled by the negative charge of the polymer surface, and no association will take place readily. However, it is well established that regardless of the nature of molecules, both electrostatic and hydrophobic interactions contribute to nanoparticle surfactant association to different extents. Thus, when a nanoparticle has charged moieties spreading along the length of the polymer chain, the
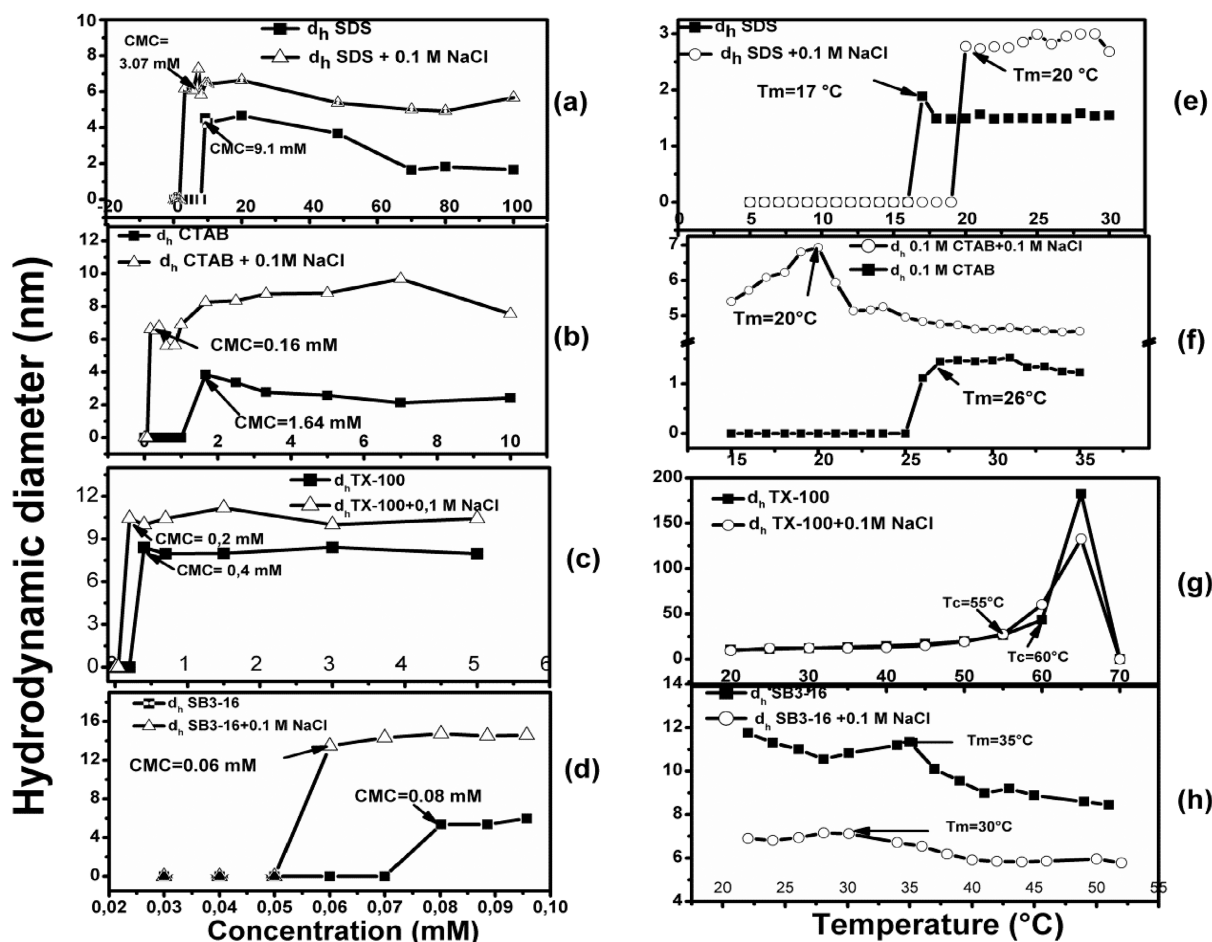
Figure 2. Evolution of the hydrodynamic diameter of surfactants (a, e) SDS, (b, f) CTAB, (c, g) TX-100 (at 298 K), and (d, h) SB3-16 (at 313 K) versus concentration (a−d) or temperature (e−h) with and without 0.1 M NaCl.

Table 2. Values of Different Thermodynamic Parameters of Surfactants without NaCl and with 0.1 M NaCl at 298 and 313 K for SB3-16

surfactant + salt		CMC (mM)	T_k (°C)	T_m (°C)	T_c (°C)
SDS	0 M NaCl	9.1; 8.3[18]		16; 17[21] (DLS)	
	0.1 M NaCl	3.07		20; 20[21] (DLS)	
	polystyrene	7.87	8	15	
CTAB	0 M NaCl	1.64; 0.82[19]		25; 25[18] (tensiometry)	
	0.1 M NaCl	0.16		20	
	polystyrene	1.2	21	26	
TX-100	0 M NaCl	0.4; 0.41[20]			60; 65[16]
	0.1 M NaCl	0.2			55; 60[16]
	polystyrene	0.19			60
SB3-16	0 M NaCl	0.08		35	
	0.1 M NaCl	0.06		30	
	polystyrene	0.01	32	38	

electrostatic interaction may be weakened by primary adsorption of the counterions, giving the hydrophobic interaction more weight in the balance of forces,[34−37] especially if the surfactant hydrophobic chain is long enough.[38−41]

For the CTAB case in Figure 3b, the initial negative charge of the polystyrene nanoparticle decreases and becomes positive

because the CTAB surfactants are positively charged. In fact, at low surfactant-to-polymer ratio, the particles are thought to have the same charge as the polymer nanoparticle, but as the molar ratio is further increased and most of the solution contains a surfactant, the charge continues to evolve to the charge of the surfactant head.[42,43] So, for CTAB, it is obvious to claim that the electrostatic attraction is the dominant force that causes the adsorption of such a surfactant on the nanoparticle. From the zeta potential values at these surfactant concentrations below, the CMC one can conclude that there are enough adsorbed surfactants in terms of electric charge compared to the ones on the polymer nanoparticles, which explain the high positive charge. For TX-100 and SB3-16 surfactants in Figure 3c,d, an insignificant change in the negative charge on the polystyrene nanoparticles is observed for the latter, whereas for the former, an unexpected behavior is shown with a noticeable change in zeta potential in the concentration range of 0.1 to 0.5 mM. This may indicate that for the TX-100 case, the hydrophobic interaction is the dominant driving forces for the adsorption of these surfactants with PSNP. The overall description is that as the concentration rises, the PSNP surface coverage by surfactants expands and the z-average diameter shows a significant progressive increase, but for the zeta potential, the variation depends on the ionic nature of the surfactant, its polarity, and its interaction with the polymer hydrocarbon chain.
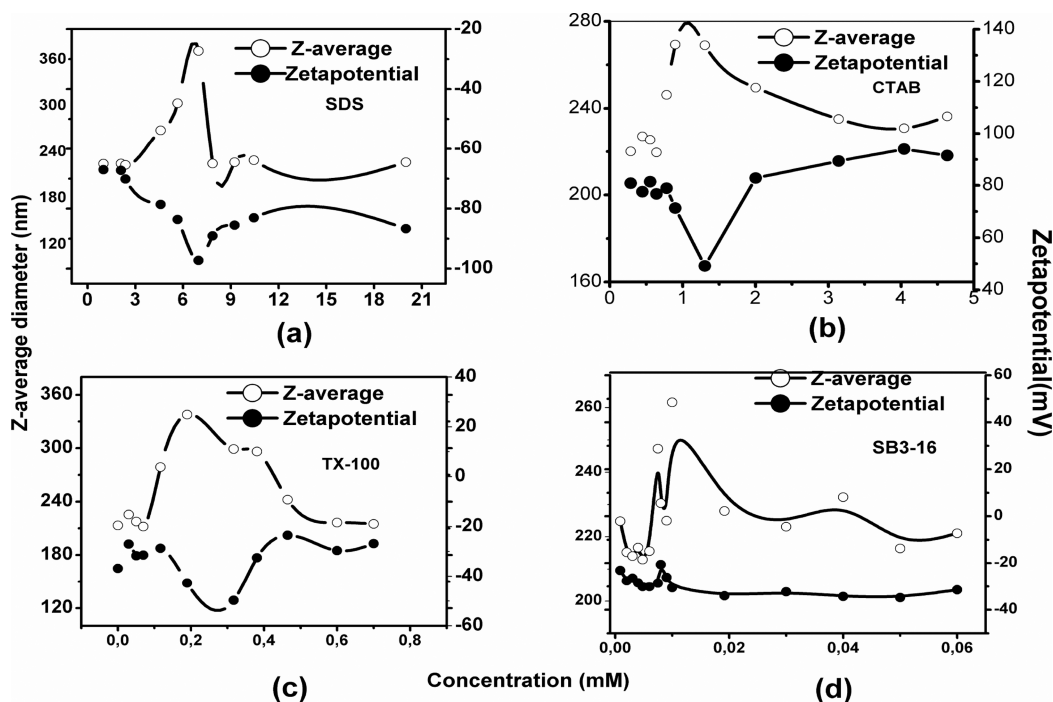
Figure 3. Variation of *z*-average diameter and zeta potential of polystyrene nanoparticle aqueous solutions versus surfactant concentration: (a) SDS, (b) CTAB, (c) TX-100, and (d) SB3-16.
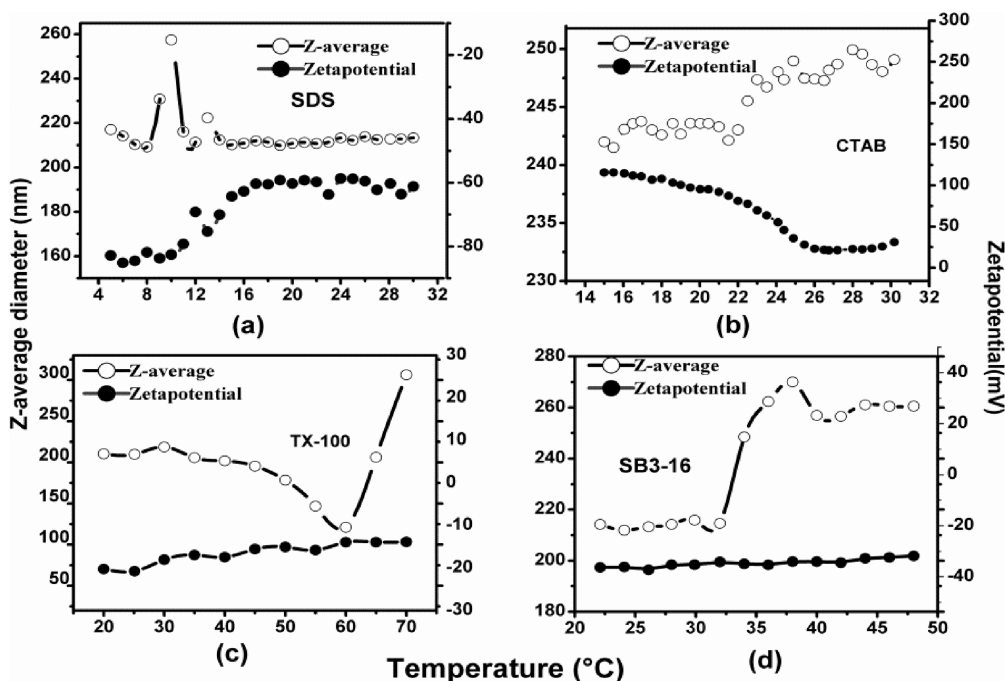

Figure 4. Variation of *z*-average diameter and zeta potential of polystyrene nanoparticle aqueous solutions versus temperature in the presence of surfactants (a) SDS, (b) CTAB, (c) TX-100, and (d) SB3-16.

As the concentration increases more, the alkyl chains of the adsorbed-surfactants can then interact more effectively together, leading to the formation of hemimicelles and further to micelles when the concentration of the surfactants in solution approaches the corresponding CMC: 8 mM for SDS, 1 mM for CTAB, 0.2 mM for TX-100, and 0.4 mM for SB3-16. From the *z*-average diameter variation, it seems that both SDS and TX-100 produce larger surfactant-adsorbed polystyrene nanoparticles and, that for SB3-16 or CTAB surfactants, the

PSNP does not increase more than 30 to 50 nm from its initial size. This behavior may indicate that both SDS and TX-100 do not interact strongly with the PSPN and prefer to self-aggregate to form micelles in the vicinity of their host nanoparticle in opposition to SB3-16 and CTAB, which interact cooperatively to PSPN at the expense of their micellization.

3.4. Effect of the Temperature of Different Surfactants on the Size Distribution of Polystyrene. The
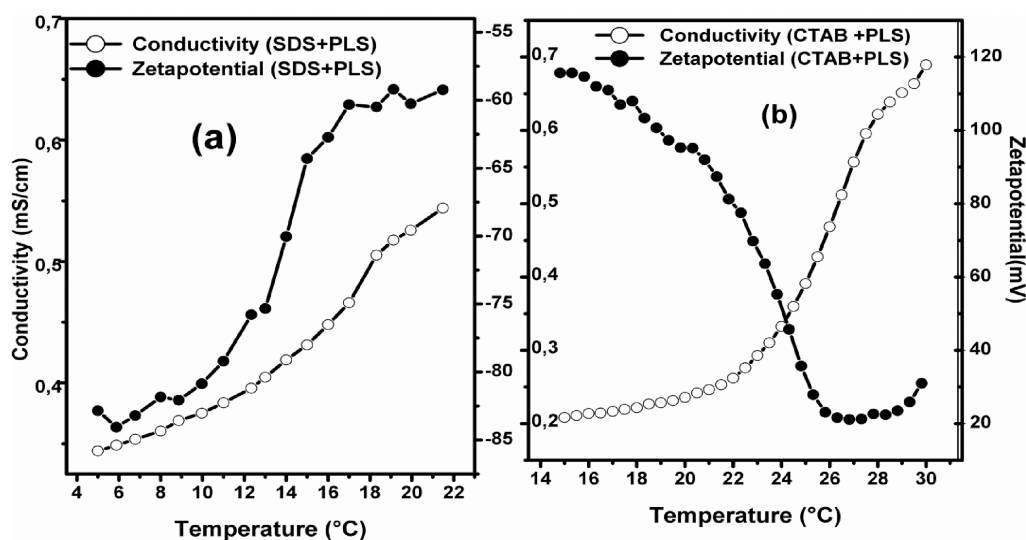
Figure 5. Variation of conductivity and zeta potential of polystyrene nanoparticle aqueous solution versus temperature in the presence of (a) SDS and (b) CTAB.

variation in the z-average diameter of the polystyrene particles dissolved in aqueous surfactant solutions above their corresponding CMC as a function of temperature and the related change in the zeta potential are shown in Figure 4a−d for SDS, CTAB, TX-100, and SB3-16, respectively. To avoid any confusion, we recall that the temperature effect was studied with surfactant solutions whose concentration is 10 times greater than the CMC. This is necessary to be able to follow the phase transition temperatures.

The changes in zeta potential and z-average diameter evolve almost simultaneously with temperature variation similar to those obtained with the concentration effect. These results are the consequence of the variability of the surfactant's environment as the temperature increases. It is worth noting to keep in mind that during the temperature increase, the surfactants are subject to different chemical and physical equilibria, namely, micelle = free surfactant equilibrium, micelle = hydrated crystal equilibrium, free surfactant = hydrated crystal equilibrium, and equilibria between polystyrene nanoparticles with each chemical species present in solution at a given temperature.[2−5]

For the SDS case, the values of z-average diameter seem to slightly diminish when the temperature increases from 5 to 8 °C, revealing a weak contraction in the PSNP owing to the first adsorption stage of free surfactant molecules, as confirmed by Z_p values, which are already around −85 mV, far from the initial −45 mV of the pure PSNPs solution. From $T = 8$ °C and up, the z-average diameter increases considerably with temperature but, beyond $T = 10$ °C, starts to decrease to finally reach an approximately constant value above $T ≈ 16$ °C and remains constant above this last temperature. When the variation of zeta potential is followed above $T = 10$ °C, its value changes from −85 mV to reach a plateau at −60 mV beyond $T = 16$ °C.

Undoubtedly, the increase in the polystyrene nanoparticle z-average diameter beyond $T_k = 8$ °C is the consequence of the second stage of adsorption of free surfactant molecules released from the hydrated crystals melting. In other words, from $T = 8$ °C, which is the Krafft temperature (MAM) of SDS surfactants, the solubility increases dramatically and the excess of the released surfactant molecules has to contribute either to the polystyrene adsorption process or the micellization one.

However, it is clear that as much as the concentration of the released surfactant did not cover all PSPN particle surfaces or reach the critical micellar concentration, the PSNP diameter increases, but once the CMC is reached, the process leading to the micelle formation will be overcome. At this point around $T = 10$ °C, the hydrodynamic diameter size starts to diminish, which means that the adsorbed surfactant molecules start to desorb from the polystyrene nanoparticles toward the solution to self-associate for forming more micelle species. The desorption process is confirmed by the variation of the zeta potential, which changes from −85 to −60 mV, and the PSNP size reduction. Beyond $T_m = 16$ °C, the PSNP diameter remains constant because only the chemical equilibrium free surfactant = micelle dominates in the bulk. This scenario is corroborated by the variation of conductivity and zeta potential of the solution with temperature, as shown in Figure 5. Thus, the break points on the conductivity and zeta potential curves emphasize the phase transition temperatures ($T_k = 8$ °C and $T_m = 16$ °C).[3,4]

The same concepts may be adopted to interpret the variation of z-average diameter and zeta potential of the CTAB-PSNP system as a function of temperature with the exception that the CTAB hydrophobic tails are positively charged. So, besides the hydrophobic interaction, which always governs the primary adsorption process, the attractive electrostatic effect contributes to the strength of the adsorption process quantitatively. This may explain, on the one hand, that the z-average diameter of the CTAB-PSNP particle is relatively more extended at low temperatures compared to the one observed for SDS and, on the other hand, why the zeta potential value is so positive. On Figure 5, one can verify that the thermal conductivity variation of CTAB solution presents deviations at peculiar temperatures, i.e., at $T = 20$ °C for Krafft temperature and $T = 26$ °C for melting temperature. Zeta potential and conductivity variations in Figure 5a,b underline the utility of PSNP to detect the transition temperatures for such surfactants. It is also interesting to note that while the PSPN's size variation from $T = 20$ °C to $T = 26$ °C is very limited compared to the one reported for SDS solution, the zeta potential changes dramatically from +120 to +25 mV. This behavior may derive from the difference in attractive

electrostatic interaction between the negatively charged PSPN surface and the free surfactant-rich phase at low temperatures or the micelle-rich phase at higher ones.

For the TX-100 surfactant at ambient temperatures, the PSNP z-average diameter presents a weak contraction but is still close to the value reported for the pure PSNP. The z-average diameter begins to decrease with temperature increasing because of the dehydration process, which enhances the attraction of the hydrophobic parts. The diameter value variation reaches its minimum, which is identified as the cloud temperature at T_c = 60 °C from where phase separation occurs.[5] Zeta potential variations are negligible along the temperature range, and the observed values change from −20 to −15 mV at the phase separation onset. When the SB3-16 surfactants are studied with PSNP, we observe, at T_k = 32 °C, a clear transition where the z-average diameter increases from 215 to 270 nm, revealing surely the adsorption process of such surfactants on the PSNP. Above T_m = 38 °C, the z-average diameter values stabilized, leading to similar behavior to the one observed with CTAB surfactants. This leads us to conclude that the SB3-16 zwitterionic surfactant behaves as a cationic surfactant with regard to the adsorption on the negatively charged PSNP. Unfortunately, for both TX-100 and SB3-16 surfactants, the zeta potential variations do not bring determinant information about the transition temperatures.

4. CONCLUSIONS

The micellization process of four types of surfactants (SDS, CTAB, TX-100, and SB3-16) in aqueous solutions has been investigated by dynamic light scattering experiments at different temperatures. The results show that the hydrodynamic diameter of every studied surfactant remains merely constant in the concentration range from 1 × CMC to 10 × CMC. An increase in the ionic strength of the aqueous surfactant solutions with the addition of 0.1 M NaCl leads to a decrease in the CMC values and an increase in the micelle sizes.

Furthermore, the thermal treatment of the surfactant solutions enabled us to detect the hydrated crystal melting temperature T_m of the different ionic surfactants in the absence and presence of the NaCl salt. For CTAB and SB3-16 surfactants, the T_m values decrease with the addition of salt in opposition of the SDS surfactant, which shows an increase in T_m value, whereas a little effect is observed for pure TX-100 surfactant solution, but T_c temperature seems to shift up after NaCl addition.

Finally, when the same type of experiment was conducted in the presence of polystyrene nanoparticles instead of NaCl salt, the analysis of the variation of the polystyrene nanoparticle z-average diameter and zeta potential enabled detection of the CMC and the following of the surfactant adsorption process on the nanoparticle surface. From the thermal treatment, it was interesting to detect simultaneously the melting and Krafft temperatures and to show that the SB3-16 surfactant behaves as the cationic surfactant CTAB.

■ AUTHOR INFORMATION

Corresponding Author
Khaled O. Sebakhy − Department of Materials, Textiles and Chemical Engineering, Laboratory for Chemical Technology (LCT), University of Gent, Zwijnaarde 9052, Belgium; orcid.org/0000-0001-6620-0951;
Email: khaled.sebakhy@ugent.be

Authors
Aicha Kadiri − Laboratory of Physical Chemistry of Macromolecules and Biological Interfaces, Mustapha Stambouli University, Mascara 29000, Algeria

Teffaha Fergoug − Laboratory of Physical Chemistry of Macromolecules and Biological Interfaces, Mustapha Stambouli University, Mascara 29000, Algeria

Youcef Bouhadda − Laboratory of Physical Chemistry of Macromolecules and Biological Interfaces, Mustapha Stambouli University, Mascara 29000, Algeria

Rachida Aribi − Laboratory of Physical Chemistry of Macromolecules and Biological Interfaces, Mustapha Stambouli University, Mascara 29000, Algeria

Fatima Yssaad − Laboratory of Physical Chemistry of Macromolecules and Biological Interfaces, Mustapha Stambouli University, Mascara 29000, Algeria

Zineeddine Daikh − Laboratory of Physical Chemistry of Macromolecules and Biological Interfaces, Mustapha Stambouli University, Mascara 29000, Algeria

Mustapha El Hariri El Nokab − Zernike Institute for Advanced Materials (ZIAM), University of Groningen, Groningen 9700, The Netherlands; orcid.org/0000-0002-9211-427X

Paul H. M. Van Steenberge − Department of Materials, Textiles and Chemical Engineering, Laboratory for Chemical Technology (LCT), University of Gent, Zwijnaarde 9052, Belgium; orcid.org/0000-0001-6244-1299

Complete contact information is available at:
https://pubs.acs.org/10.1021/acsomega.3c05956

Notes
The authors declare no competing financial interest.

■ ACKNOWLEDGMENTS

■ REFERENCES

(1) Rosen, M. J.; Kunjappu, J. T. Surfactants and Interfacial Phenomena, 4th Edition.; John Wiley & Sons, Ltd: New Jersey, USA, 2012 DOI: 10.1002/9781118228920.

(2) Rhein, L. D.; Schlossman, M.; O'Lenick, A.; Somasundaran, P.Surfactants in Personal Care Products and Decorative Cosmetics, 3rd Edition; CRC Press, Taylor & Francis Group:Florida, USA, 2006; Vol. 135 DOI: 10.1201/9781420016123.

(3) Nakayama, H.; Shinoda, K. The Effect of Added Salts on the Solubilities and Krafft Points of Sodium Dodecyl Sulfate and Potassium Perfluoro-Octanoate. Bull. Chem. Soc. Jpn. 1967, 40, 1797−1799.

(4) Moroi, Y. Micelles Theoretical and Applied Aspects; Springer: New York, NY, 1992 DOI: 10.1007/978-1-4899-0700-4.

(5) Mukherjee, P.; Padhan, S. K.; Dash, S.; Patel, S.; Mishra, B. K. Clouding Behaviour in Surfactant Systems. Adv. Colloid Interface Sci. 2011, 162 (1), 59−79.

(6) Kumar, D.; Hidayathulla, S.; Rub, M. A. Association Behavior of a Mixed System of the Antidepressant Drug Imipramine Hydrochloride and Dioctyl Sulfosuccinate Sodium Salt: Effect of Temperature and Salt. J. Mol. Liq. 2018, 271, 254−264.

(7) Kumar, D.; Rub, M. A. Studies of Interaction between Ninhydrin and Gly-Leu Dipeptide: Influence of Cationic Surfactants (m-s-m Type Gemini). J. Mol. Liq. 2018, 269, 1−7.

(8) Fergoug, T.; Bendedouch, D.; Aicart, E. Characterization of the 1-Heptodecafluorodecyl-Pyridinium Iodide in Solution: Partial Phase

Diagram and Micellar Properties from Conductivity and Surface Tension. *Colloids and Surfaces A: Physicochemical and Engineering Aspects* **2004**, *237* (1−3), 95−103.

(9) Matsuki, H.; Ichikawa, R.; Kaneshina, S.; Kamaya, H.; Ueda, I. Differential Scanning Calorimetric Study on the Krafft Phenomenon of Local Anesthetics. *J. Colloid Interface Sci.* **1996**, *181* (2), 362−369.

(10) Kroll, P.; Benke, J.; Enders, S.; Brandenbusch, C.; Sadowski, G. Influence of Temperature and Concentration on the Self-Assembly of Nonionic CiEj Surfactants: A Light Scattering Study. *ACS Omega* **2022**, *7* (8), 7057−7065.

(11) Lipfert, J.; Columbus, L.; Chu, V. B.; Lesley, S. A.; Doniach, S. Size and Shape of Detergent Micelles Determined by Small-Angle X-Ray Scattering. *J. Phys. Chem. B* **2007**, *111* (43), 12427−12438.

(12) Ogino, K.; Kubota, T.; Uchiyama, H.; Abe, M. Micelle Formation and Micellar Size by a Light Scattering Technique. *Journal of Japan Oil Chemists Society* **1988**, *37*, 588−591.

(13) Mazer, N. A.; Benedek, G. B.; Carey, M. C. An Investigation of the Micellar Phase of Sodium Dodecyl Sulfate in Aqueous Sodium Chloride Solutions Using Quasielastic Light Scattering Spectroscopy. *J. Phys. Chem.* **1976**, *80* (10), 1075−1085.

(14) Zhang, W.; Li, G.; Mu, J.; Shen, Q.; Zheng, L.; Liang, H.; Wu, C. Effect of KBr on the Micellar Properties of CTAB. *Chin. Sci. Bull.* **2000**, *45* (20), 1854−1857.

(15) Hayashi, S.; Ikeda, S. Micelle Size and Shape of Sodium Dodecyl Sulfate in Concentrated Sodium Chloride Solutions. *J. Phys. Chem.* **1980**, *84* (7), 744−751.

(16) Rohde, A.; Sackmann, E. Quasielastic Light-Scattering Studies of Micellar Sodium Dodecyl Sulfate Solutions at the Low Concentration Limit. *J. Colloid Interface Sci.* **1979**, *70* (3), 494−505.

(17) Mirgorod, Y.; Chekadanov, A.; Dolenko, T. STRUCTURE OF MICELLES OF SODIUM DODECYL SULPHATE IN WATER: AN X-RAY AND DYNAMIC LIGHT SCATTERING STUDY. *Chem. J. Mold.* **2019**, *14* (1), 107−119.

(18) Petzold, G.; Mende, M.; Kochurova, N. Polymer−Surfactant Complexes as Flocculants. *Colloids and Surfaces A: Physicochemical and Engineering Aspects* **2007**, *298* (1), 139−144.

(19) Goddard, E. D. Polymer/Surfactant Interaction—Its Relevance to Detergent Systems. *J. Am. Oil Chem. Soc.* **1994**, *71* (1), 1−16.

(20) Goddard, E. D. Polymer/Surfactant Interaction: Interfacial Aspects. *J. Colloid Interface Sci.* **2002**, *256* (1), 228−235.

(21) Budhathoki, M.; Barnee, S. H. R.; Shiau, B.-J.; Harwell, J. H. Improved Oil Recovery by Reducing Surfactant Adsorption with Polyelectrolyte in High Saline Brine. *Colloids and Surfaces A: Physicochemical and Engineering Aspects* **2016**, *498*, 66−73.

(22) Bradbury, R.; Penfold, J.; Thomas, R. K.; Tucker, I. M.; Petkov, J. T.; Jones, C. Manipulating Perfume Delivery to the Interface Using Polymer−Surfactant Interactions. *J. Colloid Interface Sci.* **2016**, *466*, 220−226.

(23) Chiappisi, L.; Hoffmann, I.; Gradzielski, M. Complexes of Oppositely Charged Polyelectrolytes and Surfactants − Recent Developments in the Field of Biologically Derived Polyelectrolytes. *Soft Matter* **2013**, *9* (15), 3896−3909.

(24) Shulevich, Y. V.; Nguyen, T. H.; Tutaev, D. S.; Navrotskii, A. V.; Novakov, I. A. Purification of Fat-Containing Wastewater Using Polyelectrolyte−Surfactant Complexes. *Separation and Purification Technology* **2013**, *113*, 18−23.

(25) Lindman, B.; Antunes, F.; Aidarova, S.; Miguel, M.; Nylander, T. Polyelectrolyte-Surfactant Association—from Fundamentals to Applications. *Colloid J.* **2014**, *76* (5), 585−594.

(26) Lapitsky, Y.; Parikh, M.; Kaler, E. W. Calorimetric Determination of Surfactant/Polyelectrolyte Binding Isotherms. *J. Phys. Chem. B* **2007**, *111* (29), 8379−8387.

(27) McNeil-Watson, F.; Tscharnuter, W.; Miller, J. A New Instrument for the Measurement of Very Small Electrophoretic Mobilities Using Phase Analysis Light Scattering (PALS). *Colloids and Surfaces A: Physicochemical and Engineering Aspects* **1998**, *140* (1−3), 53−57.

(28) Mahbub, S.; Rub, M. A.; Hoque, A.; Khan, M. A.; Asiri, A. M. Critical Micelle Concentrations of Sodium Dodecyl Sulfate and

Cetyltrimethylammonium Bromide Mixtures in Binary Mixtures of Various Salts at Different Temperatures and Compositions. *Russ. J. Phys. Chem. A* **2019**, *93* (10), 2043−2052.

(29) Molina-Bolívar, J. A.; Aguiar, J.; Ruiz, C. C. Growth and Hydration Of Triton X-100 Micelles In Monovalent Alkali Salts: A Light Scattering Study. *J. Phys. Chem. B* **2002**, *106* (4), 870−877.

(30) Thakkar, K.; Bharatiya, B.; Shah, D. O.; Bahadur, P. Investigations on Zwitterionic Alkylsulfobetaines and Nonionic Triton X-100 in Mixed Aqueous Solutions: Effect on Size, Phase Separation and Mixed Micellar Characteristics. *J. Mol. Liq.* **2015**, *209*, 569−577.

(31) Mirgorod, Y. A.; Dolenko, T. A. Liquid Polyamorphous Transition and Self-Organization in Aqueous Solutions of Ionic Surfactants. *Langmuir* **2015**, *31* (31), 8535−8547.

(32) Thakkar, K.; Bharatiya, B.; Shah, D. O.; Ray, D.; Aswal, V. K.; Bahadur, P. Interaction of Ionic Liquid Type Cationic Surfactants with Triton X-100 Nonionic Micelles. *Colloids and Surfaces A: Physicochemical and Engineering Aspects* **2015**, *484*, 547−557.

(33) Roy, J. C.; Islam, Md. N.; Aktaruzzaman, G. The Effect of NaCl on the Krafft Temperature and Related Behavior of Cetyltrimethyl-lammonium Bromide in Aqueous Solution. *Journal of Surfactants and Detergents* **2014**, *17* (2), 231−242.

(34) Bain, C. D.; Claesson, P. M.; Langevin, D.; Meszaros, R.; Nylander, T.; Stubenrauch, C.; Titmuss, S.; von Klitzing, R. Complexes of Surfactants with Oppositely Charged Polymers at Surfaces and in Bulk. *Adv. Colloid Interface Sci.* **2010**, *155* (1−2), 32−49.

(35) Liu, Z. H.; Lv, W. J.; Zhao, S. L.; Shang, Y. Z.; Peng, C. J.; Wang, H. L.; Liu, H. L. Effects of the Hydrophilicity or Hydrophobicity of the Neutral Block on the Structural Formation of a Block Polyelectrolyte/Surfactant Complex: A Molecular Dynamics Simulation Study. *Computational Condensed Matter* **2015**, *2*, 16−24.

(36) Koetz, J.; Kosmella, S. *Polyelectrolytes and Nanoparticles*; Springer-Verlag Berlin: Heidelberg, 2007 DOI: 10.1007/978-3-540-46382-5.

(37) Guzmán, E.; Llamas, S.; Maestro, A.; Fernández-Peña, L.; Akanno, A.; Miller, R.; Ortega, F.; Rubio, R. G. Polymer−Surfactant Systems in Bulk and at Fluid Interfaces. *Adv. Colloid Interface Sci.* **2016**, *233*, 38−64.

(38) Brown, W.; Zhao, J. Adsorption of Sodium Dodecyl Sulfate on Polystyrene Latex Particles Using Dynamic Light Scattering and Zeta Potential Measurements. *Macromolecules* **1993**, *26* (11), 2711−2715.

(39) Nilsson, S.; Blokhus, A. M.; Hellebust, S.; Glomm, W. R. Influence of Hydrophobic Cosolutes on the Associative/Segregative Phase Separation of Aqueous Cationic Surfactant−Polymer Systems. *Langmuir* **2002**, *18* (17), 6504−6506.

(40) Lee, N.; Thirumalai, D. Dynamics of Collapse of Flexible Polyelectrolytes in Poor Solvents. *Macromolecules* **2001**, *34* (10), 3446−3457.

(41) Nizri, G.; Magdassi, S.; Schmidt, J.; Cohen, Y.; Talmon, Y. Microstructural Characterization of Micro- and Nanoparticles Formed by Polymer−Surfactant Interactions. *Langmuir* **2004**, *20* (11), 4380−4385.

(42) Nizri, G.; Lagerge, S.; Kamyshny, A.; Major, D. T.; Magdassi, S. Polymer−Surfactant Interactions: Binding Mechanism of Sodium Dodecyl Sulfate to Poly(Diallyldimethylammonium Chloride). *J. Colloid Interface Sci.* **2008**, *320* (1), 74−81.

(43) Pojják, K.; Bertalanits, E.; Mészáros, R. Effect of Salt on the Equilibrium and Nonequilibrium Features of Polyelectrolyte/Surfactant Association. *Langmuir* **2011**, *27*, 9139−9147.